Supporting Information for

On the Influence of the Bridge on Triplet State Delocalization in Linear Porphyrin Oligomers

Sabine Richert,[1]* Bart Limburg,[2] Harry L. Anderson,[2] and Christiane R. Timmel[1]*

[1] *Centre for Advanced Electron Spin Resonance (CAESR), Department of Chemistry, University of Oxford, South Parks Road, Oxford, OX1 3QR, United Kingdom.*

[2] *Chemistry Research Laboratory, Department of Chemistry, University of Oxford, 12 Mansfield Road, Oxford, OX1 3TA, United Kingdom.*

* E-mail: sabine.richert@chem.ox.ac.uk; christiane.timmel@chem.ox.ac.uk

Table of Contents

List of Figures

1 Synthetic Procedures

Unless stated otherwise, all reagents were obtained from commercial sources and used as received without further purification. DCM and $CHCl_3$ were dried over 4 Å molecular sieves. Petroleum ether (PE) of a 40−60 °C boiling point range was used. *N*-Bromosuccinimide was recrystallized from boiling water. Porphyrin monomer **P1$_H$** was synthesized according to a literature procedure.[1] Preparative recycling GPC was performed on a Shimadzu LC-20AD liquid chromatograph with a Shimadzu SPD-M20A diode array detector. The chromatograms were analysed in real-time using Shimadzu LabSolutions software. The eluent (toluene/pyridine 100:1) was degassed using a Shimadzu DGU-20A3R degassing unit. The samples were separated on a JAIGEL H-P pre-column, a JAIGEL 3H (20 mm×600 mm) and a JAIGEL 4H column (20 mm×600 mm) connected in series. Sample collection or recycling was switched using a Shimadzu FCV-20AH2 valve unit.

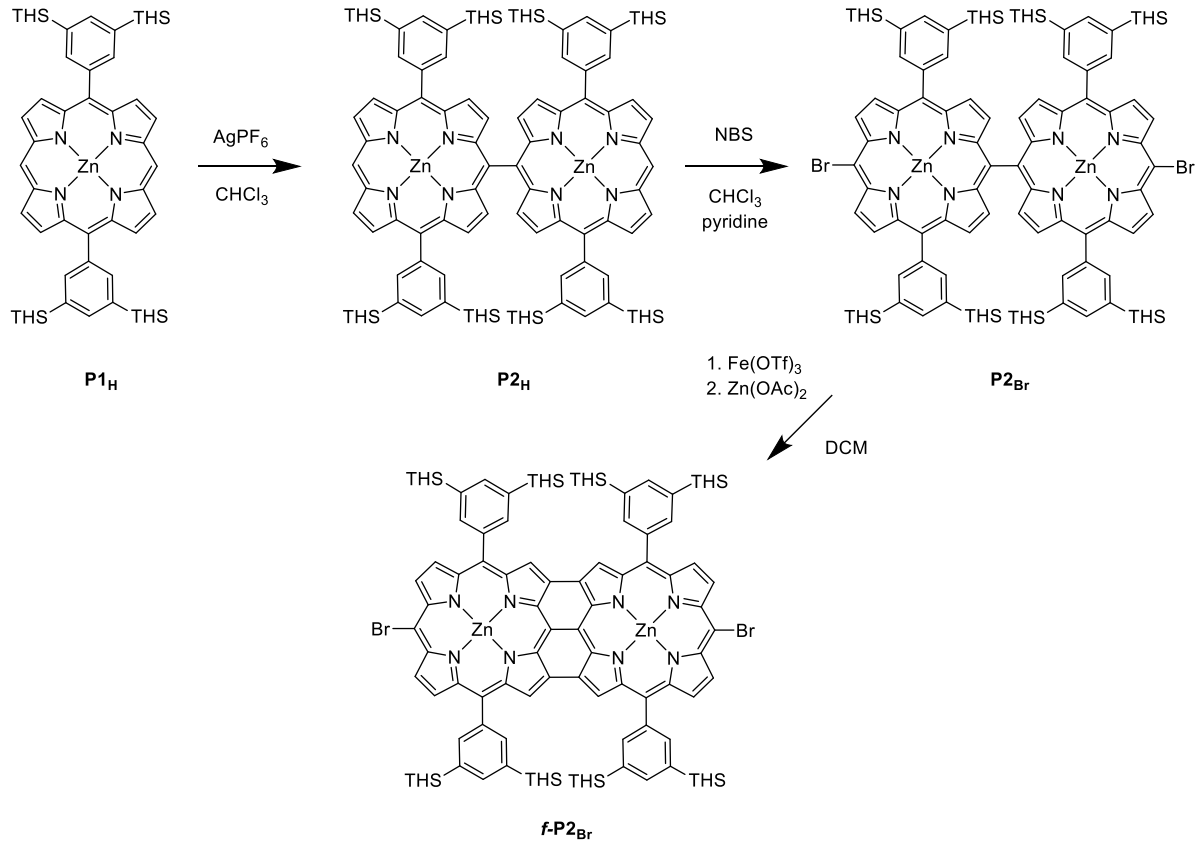

P2$_H$ and **P3$_H$**. A modified literature procedure was used for the syntheses of these compounds.[2] Compound **P1$_H$** (450 mg, 270 μmol) was dissolved in dry $CHCl_3$ (100 mL) and $AgPF_6$ (137 mg, 540 μmol) was added. The mixture heated to 50°C for 20 hours after which it was concentrated under reduced pressure. Separation of the starting material **P1$_H$** (pink) and dimer **P2$_H$** (red-brown) from the oligomers **P3$_H$**−**P6$_H$** (brown) and polymers was achieved by column chromatography (SiO_2, PE/DCM 19:1) followed by size-exclusion chromatography (Biorad Bio beads SX-1, toluene/pyridine 100:1). The brown band containing the oligomers was then subjected to recycling GPC to separate **P3$_H$** from oligomeric products. If demetallation was observed (by ^{1}H NMR peaks around −3 ppm), the isolated compounds were dissolve in $CHCl_3$ (10 mL) and 10 equivalents of

$Zn(OAc)_2$ in MeOH (1 mL) was added. After stirring for 1 hour at RT, the product was isolated by a SiO_2 plug eluting with PE/DCM 9:1.

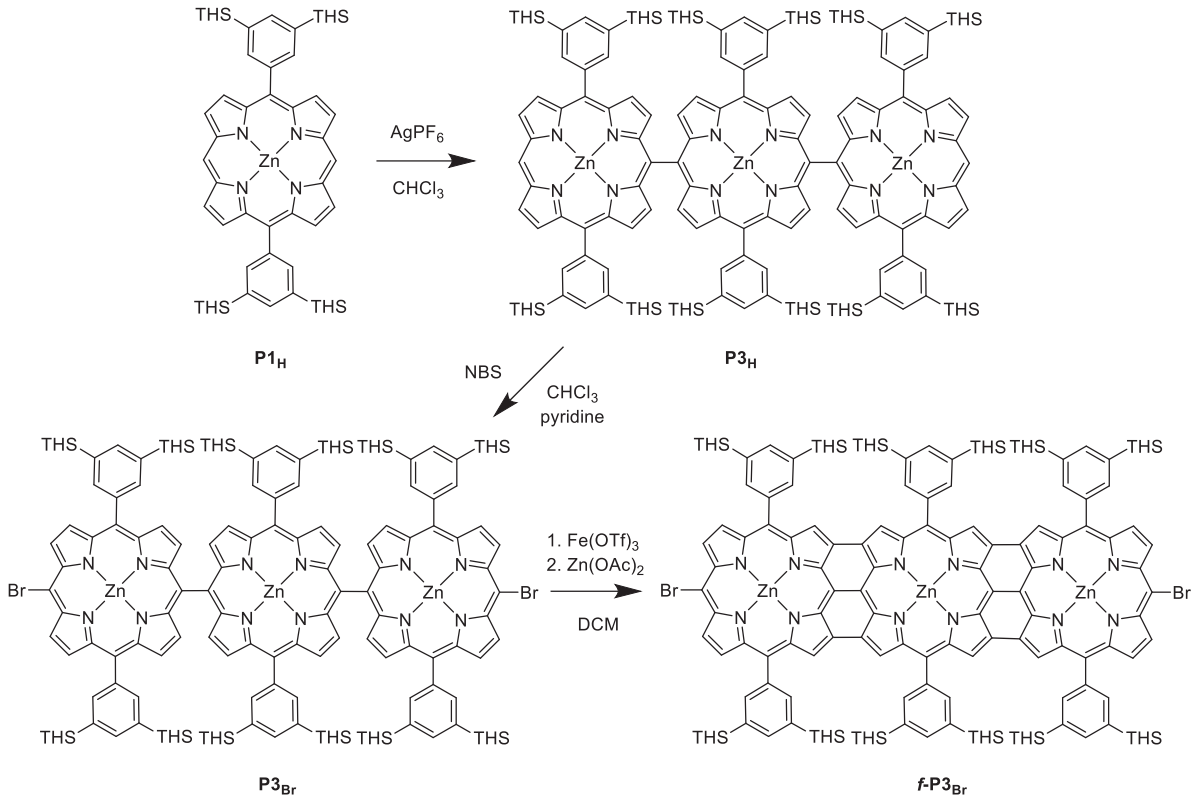

P2$_H$. Yield: 67 mg, 14 %. **^{1}H NMR** (400 MHz, $CDCl_3$, 298 K): δ_H (ppm) 10.23 (s, 2H, *meso*-H+*meso*'-H), 9.37 (d, $J = 4.5$ Hz, 4H, β-H), 8.98 (d, $J = 4.5$ Hz, 4H, β-H), 8.54 (d, $J = 4.7$ Hz, 4H, β-H), 8.41−8.21 (s, 8H, *o*-ArH), 7.85 (m, 8H, *p*-ArH + β-H), 1.72−0.52 (m, 312H, THS-H).

^{13}C NMR (101 MHz, $CDCl_3$, 298 K): δ_H (ppm) 150.90, 149.64, 141.63, 140.60, 138.73, 136.02, 134.35, 133.73, 132.26, 131.45, 131.26, 123.25, 33.57, 31.65, 24.09, 22.67, 14.16, 12.72.

MALDI-TOF (dithranol): m/z = 3311.39 (M^+ calcd. 3310.38).

UV-vis $\lambda_{max}(CHCl_3)$ / nm (ε / $mM^{-1}\,cm^{-1}$): 553 (57.4), 448 (221), 415 (274), 352 (22.9), 301 (31.8).

P3$_H$. Yield: 25 mg, 5.4 %. **^{1}H NMR** (400 MHz, $CDCl_3$, 298 K): 10.28 (s, 2H), 9.41 (d, $J = 4.4$ Hz, 4H), 9.03 (d, $J = 4.4$ Hz, 4H), 8.66 (d, $J = 4.6$ Hz, 4H), 8.50 (d, $J = 4.7$ Hz, 4H), 8.30 (s, 8H), 8.20 (s, 4H), 8.09 (d, $J = 4.6$ Hz, 4H), 7.92 (d, $J = 4.7$ Hz, 4H), 7.89 (s, 4H), 7.72 (s, 2H), 1.47−0.25 (m, 468H).

MALDI-TOF (dithranol): m/z = 4964.88 (M^+ calcd. 4964.56).

UV-vis $\lambda_{max}(CHCl_3)$ / nm (ε / $mM^{-1}\,cm^{-1}$): 563 (112), 473 (347), 412 (482), 353 (44), 304 (54.1), 260 (34.2).

P2$_{Br}$. **P2$_H$** (67 mg, 19 μmol) was dissolved in $CHCl_3$ (40 mL) and pyridine (0.16 mL) and cooled to 0 °C. To this solution was added dropwise a solution of N-bromosuccinimide (6.9 mg, 39 μmol)

in $CHCl_3$ (10 mL) and pyridine (40 μL). The mixture was stirred for 15 minutes at 0 °C after which TLC indicated full conversion. The mixture was quenched by addition of acetone (10 mL), stirred for 5 minutes and the solvents evaporated under reduced pressure. Purification by column chromatography (SiO_2, PE/pyridine 98:2) gave **P2$_{Br}$ · 2 py** as a brown solid. The coordinating pyridine was removed by flash chromatography using PE/DCM 9:1 as eluent. Yield: 99 % (69.6 mg, 19.1 μmol).

^{1}H NMR (400 MHz, $CDCl_3$, 298 K): δ_H (ppm) 9.75 (d, $J = 4.7$ Hz, 4H, β-H), 8.88 (d, $J = 4.7$ Hz, 4H, β-H), 8.47 (d, $J = 4.7$ Hz, 4H, β-H), 8.32−8.07 (m, 8H, *o*-ArH), 7.86 (s, 4H, *p*-ArH), 7.82 (d, $J = 4.7$ Hz, 4H, β-H), 1.47−0.47 (m, 312H, THS-H).

^{13}C NMR (101 MHz, $CDCl_3$, 298 K): δ_H (ppm) 155.17, 151.40, 150.12, 149.52, 141.23, 140.46, 138.95, 134.53, 133.90, 133.04, 132.47, 131.99, 123.34, 122.78, 33.57, 31.65, 24.08, 22.67, 14.16, 12.70.

MALDI-TOF (dithranol): m/z = 3466.78 (M^+ calcd. 3468.20).

UV-vis $\lambda_{max}(CHCl_3)$ / nm (ε / $mM^{-1}\,cm^{-1}$): 604 (11.3), 562 (67.8), 457 (297), 424 (293), 346 (24.3), 306 (32.8), 262 (21.7).

P3$_{Br}$. **P3$_H$** (3.4 mg, 0.69 μmol) was dissolved in $CHCl_3$ (10 mL) containing 1 % v/v pyridine. The solution was cooled down to −78 °C and to the solution was added NBS as a solution in $CHCl_3$ (1 mL) containing 1 % v/v pyridine (1 mL, 1.4 mM). The solution was stirred at −78 °C for 5 minutes and then allowed to warm to 0 °C and stirred for 1 hour. Afterwards, acetone (0.5 mL) was added and the mixture stirred for another 15 minutes at 0 °C. The solvents were removed and the residue passed over a short silica column eluting with 19:1 PE/DCM. The first eluting brown fraction afforded **P3$_{Br}$**. If NMR proved starting material was still present, more NBS was added as described above. Yield: 0.9 mg, 26 %.

^{1}H NMR (400 MHz, $CDCl_3$, 298 K): δ_H (ppm) 9.73 (d, $J = 4.7$ Hz, 4H), 8.87 (d, $J = 4.7$ Hz, 4H), 8.52 (d, $J = 4.6$ Hz, 4H), 8.48 (d, $J = 4.7$ Hz, 4H), 8.18 (s, 8H), 8.14 (s, 4H), 7.99 (d, $J = 4.5$ Hz, 4H), 7.92 (d, $J = 4.6$ Hz, 4H), 7.81 (s, 4H), 7.67 (s, 2H), 1.40−0.30 (m, 468H).

MALDI-TOF (dithranol): m/z = 5121.71 (M^+ calcd. 5122.38).

UV-vis $\lambda_{max}(CHCl_3)$ / nm (ε / $mM^{-1}\,cm^{-1}$): 566 (129), 474 (339), 422 (467), 353 (57.2), 308 (69.1), 261 (48.3).

***f*-P2$_{Br}$**. A modified literature procedure was used for the synthesis of this compound.[2] **P2$_{Br}$** (167 mg, 48.2 μmol) was dissolved in dry DCM (50 mL). To this solution was added $Fe(OTf)_3$ (122 mg, 243 μmol) as a solid. The solution was stirred for 6 hours under an argon atmosphere after which a methanolic solution of $Zn(OAc)_2$ (89 mg, 0.48 mmol in 2 mL MeOH) was added. After stirring for 30 minutes, the solvents were removed and the mixture loaded on a silica column. The starting material was removed by eluting with PE and the product eluted with PE/DCM 8:2. The fused porphyrin dimer ***f*-P2$_{Br}$** was obtained as a purple solid in 72 % yield (120 mg).

The compound was further purified by applying the same reaction conditions to the product: impure ***f*-P2$_{Br}$** (11.1 mg, 3.2 μmol) was dissolved in dry DCM (10 mL) and $Fe(OTf)_3$ (8.05 mg,

16 μmol) was added as a solid. The solution was stirred for 30 minutes after which a methanolic solution of $Zn(OAc)_2$ (1 mL, 50 mM) was added and the solution stirred further for 30 minutes. Double column chromatography (PE/DCM 9:1) yielded 10.6 mg of further purified ***f*-P2$_{Br}$** (96 %).

^{1}H NMR (400 MHz, $CDCl_3$, 298 K): δ_H (ppm) 8.55 (d, J = 4.7 Hz, 4H), 7.85 (s, 12H), 7.55 (d, J = 4.7 Hz, 4H), 7.30 (s, 4H), 1.52−0.73 (m, 312H).

MALDI-TOF (dithranol): m/z = 3464.25 (M^+ calcd. 3464.21).

UV-vis $\lambda_{max}(CHCl_3)$ / nm (ε / $mM^{-1}\,cm^{-1}$): 1046 (33.6), 920 (17.8), 565 (123), 458 (57.4), 422 (159), 355 (29.3), 258 (28.4).

***f*-P3$_{Br}$**. A modified literature procedure was used for the synthesis of this compound.[2] **P3$_{Br}$** (4.0 mg, 0.78 μmol) was dissolved in dry DCM (10 mL). To this solution was added $Fe(OTf)_3$ (3.93 mg, 7.81 μmol) as a solid. The mixture was stirred for 1 hour after which a methanolic solution of $Zn(OAc)_2$ (0.5 mL, 160 mM) was added and the mixture stirred further for 30 minutes. The mixture was purified over a SiO_2 plug and the above steps repeated two more times. After which, the product was purified by SiO_2 chromatography (PE/DCM 9:1) to give ***f*-P3$_{Br}$** (3.01 mg, 75 %).

^{1}H NMR (400 MHz, $CDCl_3$, 298 K): δ_H (ppm) 8.48 (d, J = 4.7 Hz, 4H, β_1), 7.74 (s, 4H, *o*-Ar inner), 7.71 (s, 8H, *o*-Ar outer), 7.66 (s, 2H, *p*-Ar inner), 7.53 (s, 4H, *p*-Ar outer), 7.45 (d, J = 4.7 Hz, 4H, β_2), 7.11 (s, 4H, β_3), 6.38 (s, 4H, β_4).

MALDI-TOF (dithranol): m/z = 5114.43 (M^+ calcd. 5114.32).

UV-vis $\lambda_{max}(CHCl_3)$ / nm (ε / $mM^{-1}\,cm^{-1}$): 1332 (140), 1142 (38.9), 720 (60.8), 670 (186), 591 (62.6), 424 (160), 348 (42.7), 254 (43.7).

1.1 UV-vis of Fused Compounds

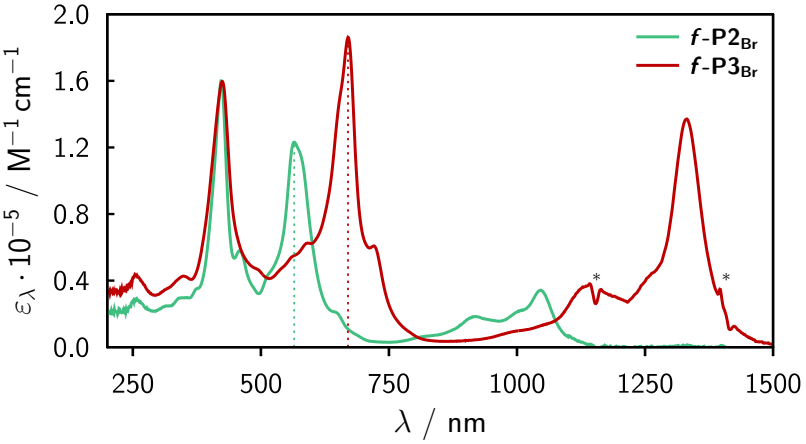

Figure S1: Comparison of the UV-vis spectra of ***f*-P2$_{Br}$** and ***f*-P3$_{Br}$**. The excitation wavelengths chosen for the acquisition of the EPR spectra are indicated by dotted lines and the asterisks indicate noise arising from imperfect subtraction of absorption bands from the solvent.

2 EPR Setup

In all EPR experiments 2-methyltetrahydrofuran (MTHF) was used as the solvent. The inhibitor-free solvent (Sigma-Aldrich, anhydrous, $\geq$99 %) was passed over a column of activated aluminium oxide to remove any traces of water and possibly formed peroxides prior to sample preparation. Solutions with a concentration of 0.1 mM or 0.2 mM were prepared and degassed in 3.8 mm OD EPR tubes (several freeze-pump-thaw cycles). The degassed solutions were frozen in liquid nitrogen and directly inserted into the EPR resonator cooled to 20 K. All experiments were carried out on a Bruker ELEXSYS E680 spectrometer operated at X-band frequencies (9.75 GHz) using a Bruker MD4 resonator (EN 4118X-MD4) equipped with RF coils. The temperature was held constant at 20 K using a helium gas-flow cryostat. The samples were excited with depolarised light at either 530 nm, 565 nm or 670 nm using a nominal excitation energy between 2 and 3 mJ at a repetition rate of 20 Hz (pulse duration 5 ns).

2.1 Transient cw EPR

The transient cw EPR spectra were acquired in direct detection mode using the transient recorder and a microwave power of 0.2 mW. Any positive signal thus corresponds to an absorptive transition and any negative signal to an emissive one. After data acquisition, the 2D spectra were baseline corrected in both dimensions using a home-written MATLAB routine. The shape of the transient cw EPR spectra was found not to change significantly over the course of the triplet state lifetime. The spectra were averaged over a time window from 0.2 to 1 μs after the laser pulse for the monomer, and from 0.04 to 0.14 μs for the tapes.

2.2 Mims ENDOR

Proton Mims ENDOR spectra were acquired using the pulse sequence $\frac{\pi}{2} - \tau - \frac{\pi}{2} - T - \frac{\pi}{2} - \tau$ and a microwave pulse length of 16 ns. Between the second and third pulse of the stimulated echo pulse sequence (i.e. during the delay T) a 15 μs RF pulse was applied. The RF power was adjusted based on a nutation experiment such that the flip angle corresponded to π. The integrated echo intensity was then monitored as a function of the RF frequency in a range centered about the ^{1}H Larmor frequency at the respective field position. For every chosen field position, three spectra with different τ values of 120, 180, and 240 ns were recorded to compensate for blind spots and added to yield the spectra shown.

3 TREPR on Tapes

Within experimental error, the decay of the dimer (***f*-P2$_{Br}$**) and trimer (***f*-P3$_{Br}$**) tape signal in transient cw mode are identical and amount to 500 ns under the applied conditions as can be seen for ***f*-P3$_{Br}$** in **Figure S2**.

Judged by the relative signal strength observed in the experiments, the triplet yield of the trimer tape seems to be at least an order of magnitude lower than that of the dimer tape. The triplet state lifetime of the dimer tape, is several orders of magnitude shorter than that of the corresponding monomer[3] and spin relaxation is faster. In addition, the triplet yield is lower.[3] The spectra for

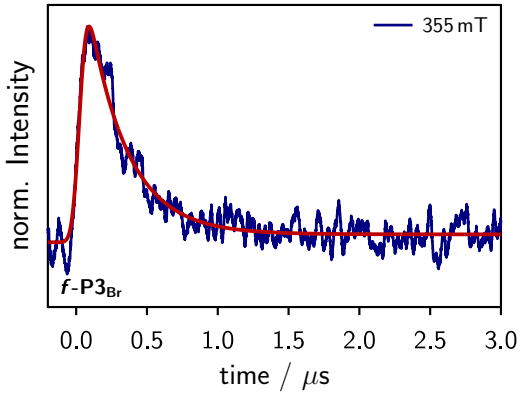

Figure S2: Decay of the transient cw EPR signal of ***f*-P3$_{Br}$** at 355 mT. A monoexponential fit yields $\tau =$ 500 ns.

the dimer and trimer tapes therefore had to be averaged for more than a day; a single scan as performed for the monomer yields no discernible triplet EPR signal. Some minor 'impurities' (i.e., intermediates of the synthesis) of monomer and dimer-like species are present in the ***f*-P3$_{Br}$** sample as can be seen from the figure (*right*, 530 nm excitation). Since the triplet signal of any such 'impurities' is potentially orders of magnitude higher, even contributions of $\ll 1\,\%$ might be visible in the spectra. Selective excitation of only the trimer tape contribution at 670 nm allowed us to isolate the 'true' spectrum of ***f*-P3$_{Br}$** as presented in the main text.

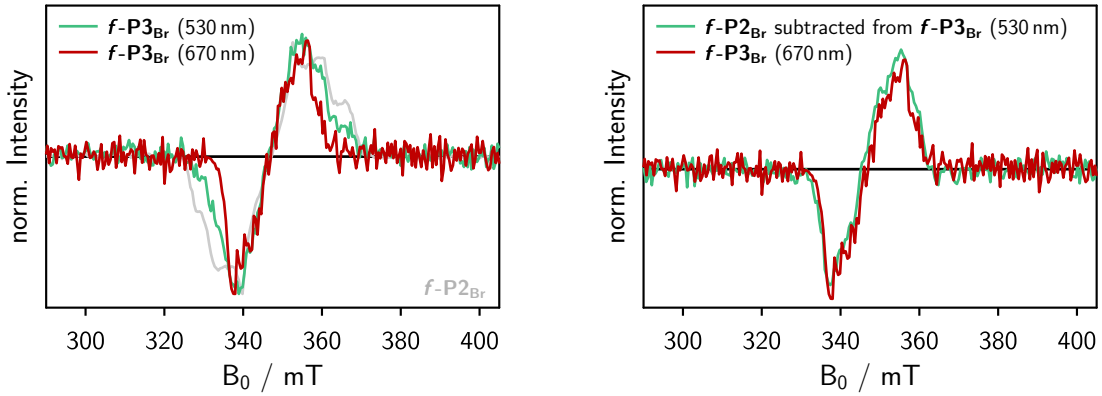

Figure S3: Comparison of the transient cw EPR spectra recorded for the ***f*-P3$_{Br}$** sample at different excitation wavelengths (*left*) and comparison of the ***f*-P3$_{Br}$** spectrum at 530 nm excitation after subtracting a dimeric contribution (scaled spectrum of ***f*-P2$_{Br}$**) with the spectrum of ***f*-P3$_{Br}$** excited at 670 nm (*right*). At 670 nm, only ***f*-P3$_{Br}$** absorbs, whereas at 530 nm also monomer or dimer-like species might absorb and contribute to the signal. The good agreement between the two spectra displayed in the right-hand panel confirms i) the presence of dimer-like 'impurities' and ii) the shape of the 'true' trimer spectrum obtained when exciting at 670 nm.

No echo signal could be detected for the tapes in pulse mode due to the very weak triplet signal. In addition, the short triplet state lifetime[3] would prevent any ENDOR measurements. TREPR experiments were also attempted on ***f*-P2$_{H}$**, but no signal could be detected, in line with the expectations of a much reduced triplet yield.[3] Since the overall triplet signal decreases markedly

within the series of fused porphyrin oligomers, no spectra could be acquired for porphyrin tapes with more than three units.

4 Spectral Simulations

Numerical simulations of the transient cw EPR spectra of the singly-linked compounds (**P1$_H$**, **P2$_H$**, and **P3$_H$**) were carried out using the MATLAB[4] package EasySpin[5] in combination with a home-written MATLAB fitting routine. Since the spectra of the three compounds are almost identical, only the simulation for the trimer, **P3$_H$**, is explicitly shown in **Figure S4**. The triplet state parameters, D and E, as well as the relative populations of the triplet sublevels, obtained as a result from the fit, are indicated in the figure.

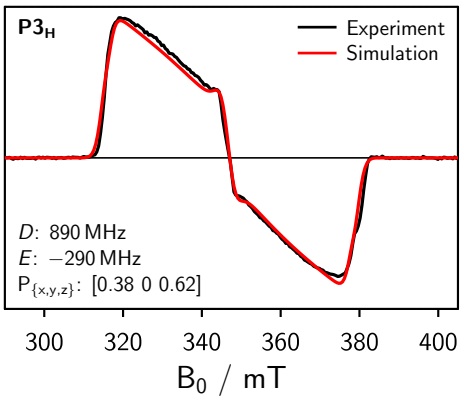

Figure S4: Numerical simulation of the triplet state cw EPR spectrum of **P3$_H$** recorded at 20 K. The ZFS parameters and relative sublevel populations are indicated in the figure.

5 Additional ENDOR Results

The TREPR spectra and ENDOR results shown below clearly confirm that the singly-linked compounds behave as monomer-like species since the largest hyperfine coupling constant remains the same in all oligomers. Localisation of the triplet state on a single porphyrin unit is observed in all cases, which confirms the tentative conclusions in reference 6 that the triplet state remains localised at dihedral angles of 90° between the porphyrin planes.

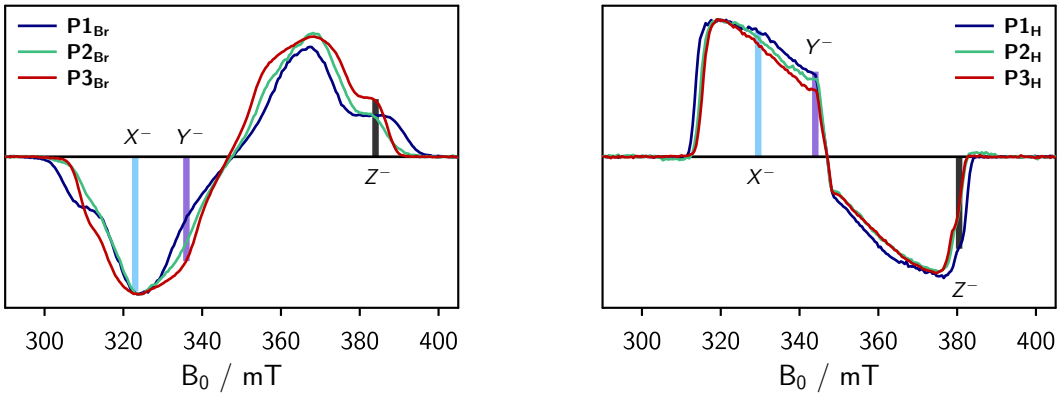

Figure S5: Transient cw EPR spectra of the singly-linked compounds with terminal −Br (*left*) and −H (*right*) groups.

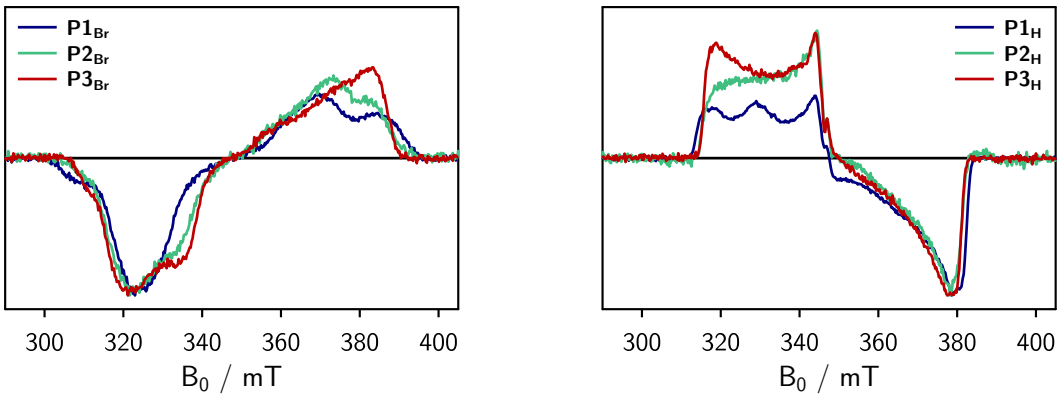

Figure S6: Field-swept echo-detected EPR spectra of the singly-linked compounds with terminal −Br (*left*) and −H (*right*) groups.

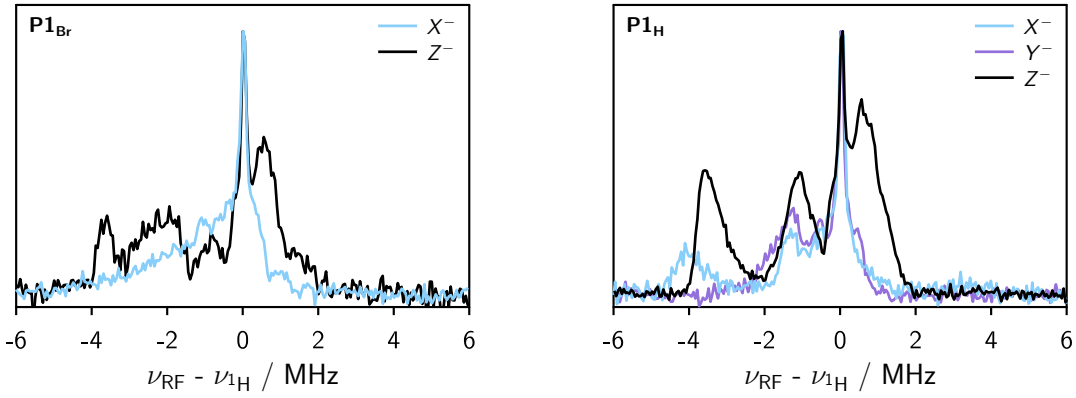

Figure S7: Proton Mims ENDOR spectra recorded at different field positions corresponding to the X, Y, and Z orientations of the ZFS tensor for $\mathbf{P1_{Br}}$ (*left*) and $\mathbf{P1_{H}}$ (*right*).

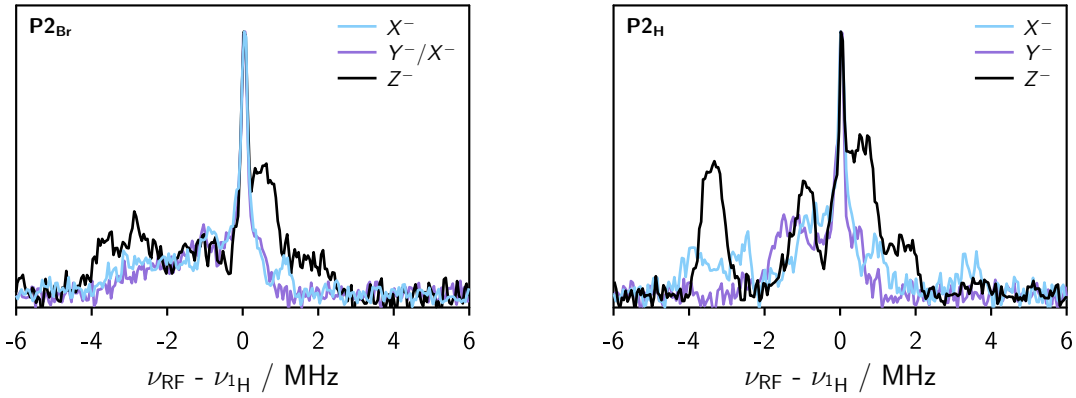

Figure S8: Proton Mims ENDOR spectra recorded at different field positions corresponding to the X, Y, and Z orientations of the ZFS tensor for $\mathbf{P2_{Br}}$ (*left*) and $\mathbf{P2_{H}}$ (*right*).

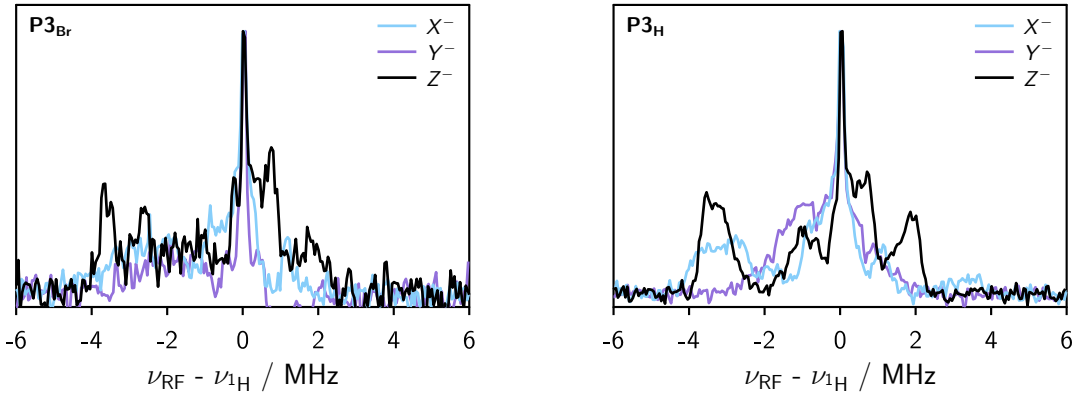

Figure S9: Proton Mims ENDOR spectra recorded at different field positions corresponding to the X, Y, and Z orientations of the ZFS tensor for $\mathbf{P3_{Br}}$ (*left*) and $\mathbf{P3_{H}}$ (*right*).

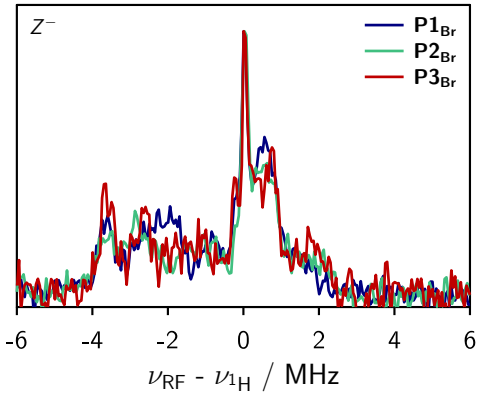

Figure S10: Comparison of the proton Mims ENDOR spectra for **P1$_{Br}$**, **P2$_{Br}$** and **P3$_{Br}$**, recorded at magnetic field positons corresponding to the Z^- orientation of the ZFS tensor.

6 DFT Calculations

Density functional theory (DFT) calculations were performed on the investigated zinc porphyrin structures in order to interpret the observed trends in the D-values. In the case of the singly-linked porphyrins, DFT also allows to assign the experimentally determined hyperfine couplings to the nuclei and to determine the orientation and magnitude of the proton hyperfine coupling tensors. The hyperfine tensors and spin densities are shown within the molecular frame.

The porphyrin structures were first optimized in Turbomole V6.1[7,8] under C_1 symmetry using DFT/B3LYP in combination with the TZVP basis set[9] and RI-approximation[10]. Frequency calculations confirmed that the obtained structures corresponded to minima of the potential energy surface.

The hyperfine interaction tensors and their orientation were then calculated for the optimized structures using the program package ORCA V3.0.[11] The ORCA DFT calculations with the B3LYP functional were performed using the EPR II basis set[12] for H, C, and N and the 6-31G(d) basis on zinc.

Table S1 shows a comparison of the experimental and calculated ZFS parameters. It is known that the D-values are considerably underestimated by DFT (often by a factor of almost two),[13] but the relative trends were generally found to be reliable in earlier work.

Table S1: Comparison of the experimental and calculated ZFS parameters.

Compound	D (exp.) / MHz	D (calc.) / MHz	$\|D\|/\|E\|$ (exp.)	$\|D\|/\|E\|$ (calc.)
P1$_{Br}$	1200	594	0.09	0.23
***f*-P2$_{Br}$**	590	346	0.13	0.23
***f*-P3$_{Br}$**	372	199	0.18	0.30

For all three compounds DFT predicts a positive D-value. The agreement between experiment and DFT is remarkable: The relative D-values in the series **P1$_{Br}$** : ***f*-P2$_{Br}$** : ***f*-P3$_{Br}$** amount to

1:0.58:0.33 in the case of DFT, whereas the experiment yields 1:0.49:0.31. The experimental *D*-values are thus in agreement with even delocalisation of the triplet state over the entire molecule in ***f*-P3$_{Br}$**, as predicted by DFT.

The DFT calculations also confirm that the singly-linked porphyrin oligomers are predicted to have a preferred dihedral angle between the porphyrin planes of 90°.

References

[1] Grozema, F. C.; Houarner-Rassin, C.; Prins, P.; Siebbeles, L. D. A.; Anderson, H. L. *J. Am. Chem. Soc.* **2007**, *129*, 13370–13371.

[2] Blake, I. M.; Krivokapic, A.; Katterle, M.; Anderson, H. L. *Chem. Commun.* **2002**, 1662–1663.

[3] McEwan, K. J.; Fleitz, P. A.; Rogers, J. E.; Slagle, J. E.; McLean, D. G.; Akdas, H.; Katterle, M.; Blake, I. M.; Anderson, H. L. *Adv. Mater.* **2004**, *16*, 1933–1935.

[4] MATLAB, *version 7.11.0 (R2010b)*; The MathWorks Inc.: Natick, Massachusetts, 2010.

[5] Stoll, S.; Schweiger, A. *J. Magn. Reson.* **2006**, *178*, 42–55.

[6] Tait, C. E.; Neuhaus, P.; Peeks, M. D.; Anderson, H. L.; Timmel, C. R. *Phys. Chem. Chem. Phys.* **2016**, *18*, 5275–5280.

[7] Ahlrichs, R.; Bär, M.; Häser, M.; Horn, H.; Kölmel, C. *Chem. Phys. Lett.* **1989**, *162*, 165–169.

[8] TURBOMOLE V6.1 2009, a development of University of Karlsruhe and Forschungszentrum Karlsruhe GmbH, 1989-2007, TURBOMOLE GmbH, since 2007; available from http://www.turbomole.com.

[9] Schäfer, A.; Huber, C.; Ahlrichs, R. *J. Chem. Phys.* **1994**, *100*, 5829–5835.

[10] Eichkorn, K.; Weigend, F.; Treutler, O.; Ahlrichs, R. *Theor. Chem. Acc.* **1997**, *97*, 119–124.

[11] Neese, F. *Wiley Interdiscip. Rev.: Comput. Mol. Sci.* **2012**, *2*, 73–78.

[12] Barone, V. In *Recent Advances in Density Functional Methods, Part I*; Chong, D. P., Ed.; World Scientific: Singapore, 1996.

[13] Neese, F. *J. Chem. Phys.* **2007**, *127*, 164112/1–9.